Wind-Tunnel Investigation of Wing-in-Ground Effects

M. D. Chawla*
Wright Research and Development Center,
Wright-Patterson Air Force Base, Ohio 45433

L. C. Edwards†
U.S. Army Safety Center,
Fort Rucker, Alabama 36362
and
M. E. Franke‡
Air Force Institute of Technology,
Wright-Patterson, Air Force Base, Ohio 45433

Wing-in-ground effects from a wind-tunnel study of a NACA 4415-profile wing model with an aspect ratio of 2.33 are described. The wing model contains a 20%-chord, full-span, adjustable flap and removable end and center plates. Ground boards are used in the wind tunnel to simulate the ground. In this study, the ground effects are expressed as variations to the aerodynamic coefficients (lift and drag) and lift-to-drag ratio. The ground effects are described in terms of angle of attack, flap angle, wing height above ground, and use and size of end and center plates. Ground effects were found to be limited to heights above the ground of one mean chord or less.

Introduction

GROUND effects experienced during takeoff and landing and flying in close proximity to the ground are widely known. Bodies tend to float when flying close to the ground. The effects can be related to the so-called "air cushion" developed in the cavity between the underside of the vehicle and the ground. In the case of a lifting surface, these effects are commonly referred to as wing-in-ground (WIG) effects.[1-3]

The research contained in this study is a part of a program directed at the development of a horizontal launch system for space-type vehicles. Usually, space vehicles are launched vertically. With more common use of the Space Shuttle system, concepts that can reduce the life-cycle costs and provide greater payload capability and flexibility are of interest. A possibility exists in the power-augmented ram, wing-in-ground effect (PAR-WIG) launcher.[1,2] This aircraft configuration has engines mounted forward of the wing so that the jet efflux can be directed under the wing to allow more lift when flying near the ground.[1,2] The PAR-WIG launcher system could be developed into a piggyback transporter, which would allow horizontal takeoff of space vehicles from conventional airfields with very short response times and be an effective platform for launching heavy payloads.[2] Gallington and Miller,[4] as well as others, have conducted studies on basic and nonpowered systems to obtain information on WIG effects. WIG studies such as these will assist in determining beneficial effects that may be available to the PAR-WIG flying mode.

The purpose of the study described herein was to select and test a wing model that would supplement work of interest to the PAR-WIG launcher efforts.[2] WIG effect studies were conducted in the 5-ft-diam wind tunnel of the Air Force Institute of Technology (AFIT). The wing model had a 20%-chord, full-span, adjustable flap, removable center and end plates, a NACA 4415 airfoil profile, and an aspect ratio of 2.33. Several parameters were varied: angle of attack, flap angle, height from ground, and the use and size of center and end plates. Objectives of the study were to determine quantitatively the ground effects in terms of the aerodynamic coefficients (lift and drag) and lift-to-drag ratio and to verify ground effect zones.

Wing Model and Apparatus

The wing model was built to match a prototype model designed for the static-table and whirling-arm-machine tests to continue the PAR-WIG research.[2,3] The model to prototype size ratio was 1/102. Design details of the wing model are given in Table 1. A photograph of the underside of the model is shown in Fig. 1.

The model was built of 1/16-in.-thick, high-strength, high-temperature casting resin with wood internal supports. Before the top was cast, wiring, tubing, and the pressure scanner were placed inside. The model had a hole at the trailing edge in the center to accommodate the sting, which also acted as a mount for the load balance. When mounted on the sting, the pitch

Table 1 Wing model design details

Wing profile	NACA 4415
Aspect ratio	2.33
Span	20.97 in.
Root chord	10.67 in.
Tip chord	7.34 in.
Mean chord, c	9.00 in.
Flap chord (0.2 c)	1.80 in.
Wing planform area	1.31 ft^2
Wing sweep angle	17.54 deg
Center and end plates	Table 3

Presented as Paper 88-2527 at the AIAA 6th Applied Aerodynamics Conference, Williamsburg, VA, June 6-8, 1989; received Aug. 26, 1988; revision received Oct. 26, 1989.

*Aerospace Engineer, Flight Dynamics Laboratory.
†Major, U.S. Army.
‡Professor, Associate Fellow AIAA.

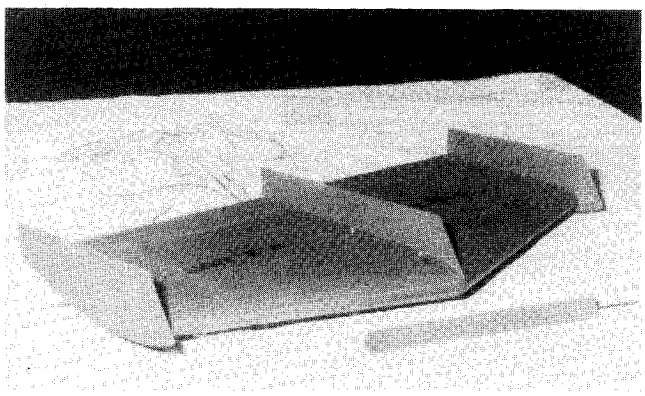

Fig. 1 Photograph of underside of wing model.

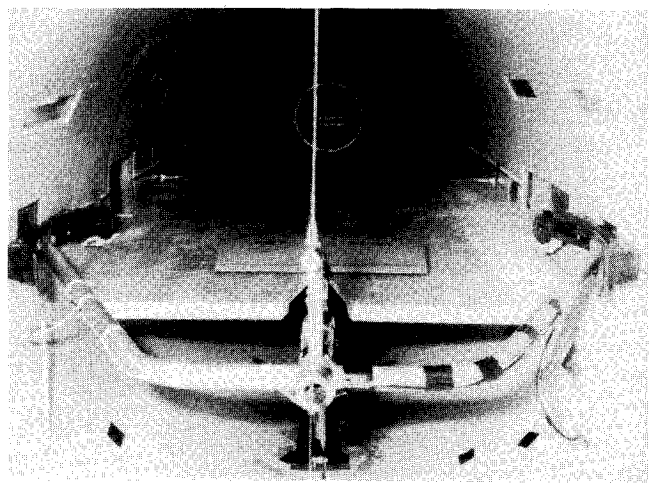

Fig. 2 Rear view of model in wind tunnel.

and yaw angles of the model could be adjusted. For these tests, the yaw angle was maintained at 0 deg.

Three different sets of plates were used on the model. Each set consisted of two end plates and one center plate all with the same height. Plate heights of 0.12, 0.15, and 0.20 c were tested to study the effect of the height of the air cushion between the wing and the ground on plate effectiveness. The profile of the plates was similar to that used on the model for the static-table and whirling-arm tests.[2] The wing flap was split at the middle to accommodate the center plate. The center plate was attached to the middle of the model from underneath and had a profile similar to the end plates except for the top edge. When the plates were attached to the model, the design was such that the model had an angle of attack of 5 deg when the bottom edges of the plates were level.

The wing model had 14 pressure taps on the left side around the mean aerodynamic chord. The tubing from each tap was connected to the pressure scanner located inside the wing. The weight of the tubing, wires, and scanner were balanced by a counterweight on the opposite side of the model. The pressure data from the scanner were fed directly into the computer.

The ground surface was simulated by flat boards. Three different boards were used that could be fitted at five different heights. Small clearances at the edges were closed by taping. The leading edges of the boards were elliptical, with a major to minor axis ratio of 4:1. Each ground board had 21 pressure taps spaced 1 in. apart along a line under the mean aerodynamic chord of the wing on one side.

The AFIT 5-ft-diam wind tunnel is open at both ends and is located inside a large building, which serves both as an inlet plenum and a discharge chamber. The flow is driven by two 12-ft counter-rotating fans and regulated by controlling the speed of the dc motors that drive the fans. The tunnel is capable of flow velocities up to approximately 300 ft/s. Total pressure is atmospheric. Static pressure is measured by manometers both upstream and downstream of the test section, and dynamic pressure is measured by a differential pressure transducer.

The design of the model was such that accounting for the ground board and the maximum pitch of the model, the blockage area was less than 7%. Thus, no corrections were made for forces and moments. A rear view of the model, sting, and ground board mounted in the tunnel is shown in Fig. 2.

Instrumentation and Data Acquisition

The mounting sting was used with a six-component strain gauge balance. The balance was mounted in the model and was calibrated for normal, side, and axial forces and pitching and rolling moments. The balance output was input to the data acquisition control unit. The data were stored on floppy disks and later converted to the aerodynamic coefficients by a computer. Each of the force component voltages from the six-component balance was sampled 10 times in approximately 2 s and then averaged at each data point.

The pressure scanners used in both the model and under the ground board were dc motor-driven pulse scanners with step controllers. Both were fitted with 2.5 psi pressure transducers with a sensitivity of 25 mV/psi. The outputs from both transducers were stored for data reduction. In addition, the measurements of dynamic pressure, temperature, barometric pressure, angle of attack, and other data were stored by the computer. Temperature was measured by a thermocouple.

Calibrations and Procedures

Initial tests were conducted to determine the flow angularity correction in the tunnel. The correction was made to determine the actual angle of attack of the wing. Angularity was determined by testing the model upright and then inverted. The angularity correction was small and depended on the ratio of the span of the model to the tunnel diameter and the amount the model was off the centerline. The angle of attack was determined from the output voltage of a rheostat connected to the electric motor that sets the angle of the model.

The ground boards in this study were fixed so that the ground was not fully simulated in the wind-tunnel tests. Thomas et al.[1] ran tests with both a stationary and a moving ground belt and found that the lift and drag coefficients below stall were not affected by the moving belt. Thus, no corrections were applied in this study for the fixed ground boards.

Before installing the model in the wind tunnel, runs were made with only the ground board. The presence of the ground board changed the dynamic pressure from the tunnel harness reading. Thus, dynamic pressure measurements were made at the model location above and below the board. The local values above the board were used for data reduction.

Each run with any board was preceded with a run using yarn tufts on the board surface to see that no undue turbulence existed at the model site. Flow visualization was also provided by oil-drop traces on the wing and the ground boards. This showed the flow pattern around the model with and without a ground board and established whether or not there was flow separation.

The pressure transducers were calibrated by applying known pressures and recording the outputs. The voltage readouts were averaged over several runs. The averaged value was used to calculate pressure and the aerodynamic coefficients.

The flow in the tunnel was maintained at a constant pressure of 10 psf or an equivalent 63 mph. The test variables were incremented gradually to study the effect of each separately and in combination with various groups. The test variables are

Table 2 Test variables[a]

Angle of attack, α	0–25 deg
Flap angle, θ	0–30 deg
Wing height, h/c	0.25, 0.5, 1.0, and 2.35

[a]Wing height was measured at c/4; c = mean chord; angles were varied in 5-deg increments.

Table 3 Plate configurations and height[a]

Center plate	End plates	Symbol[b]
None	None	OO
None	0.20 c	OL
0.20 c	0.20 c	LL
None	0.15 c	OM
0.15 c	0.15 c	MM
None	0.12 c	OS
0.12 c	0.12 c	SS

[a]Height in terms of wing mean chord c.
[b]O, S, M, and L stand for none, small-, medium-, and large-sized plates, respectively.

given in Table 2. Center and end-plate heights and configurations are given in Table 3.

Results

The lift and drag characteristics of the wing model as a function of flap angle θ with and without medium-sized center and end plates are shown in Figs. 3–5. The angle of attack α and wing height h were fixed at 5 deg and 0.25 c, respectively. The lift coefficient and drag coefficient increased with increasing flap angle, as expected. The lift coefficient of the wing with plates was approximately 15% higher than that without plates over the range of flap angles tested (see Fig. 3), whereas the effect of the plates on the drag coefficient was relatively small (see Fig. 4). The corresponding lift-to-drag ratio (see Fig. 5) also showed an increase with plates compared to that without plates because with plates C_L was higher, whereas C_D remained about the same. Thus, the plates were beneficial at $h/c = 0.25$. Tests were also run with the two other plate sizes (larger and smaller), but the results were not significantly different from those shown in Figs. 3–5. The plates were also useful at other values of h/c up to approximately $h/c = 1$, but the plates only increased the lift coefficient approximately 7% at $h/c = 0.5$ and about 4% at $h/c = 1$ for $\alpha = 5$ deg.

Tests were conducted for all three plate sizes with and without the center plate for various values of α and h/c. In all cases, the presence or absence of a center plate did not make any significant difference in the values of the aerodynamic coefficients. Although the center plate can be eliminated without any adverse effect on the aerodynamic coefficients, the presence of a center plate may be useful in other ways, such as improving the flow characteristics under the wing.

Polar plots (C_L vs C_D) for the wing model with medium-

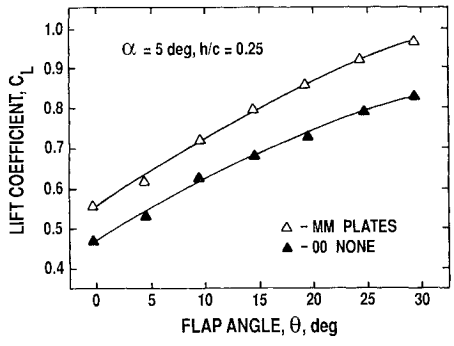

Fig. 3 Effect of plates and flap angle on lift coefficient.

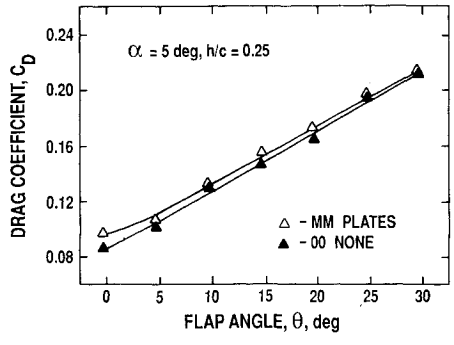

Fig. 4 Effect of plates and flap angle on drag coefficient.

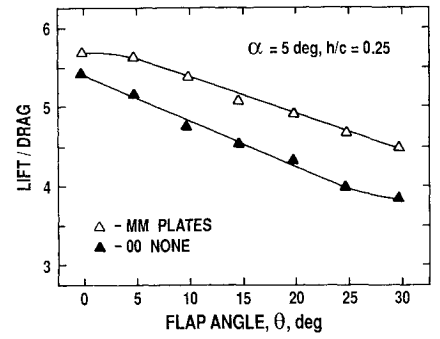

Fig. 5 Effect of plates and flap angle on lift-to-drag ratio.

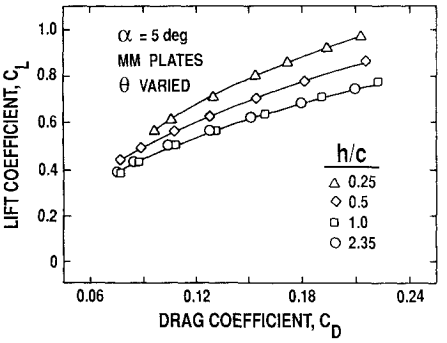

Fig. 6 Wing-in-ground effects on aerodynamic coefficients, α = 5 deg.

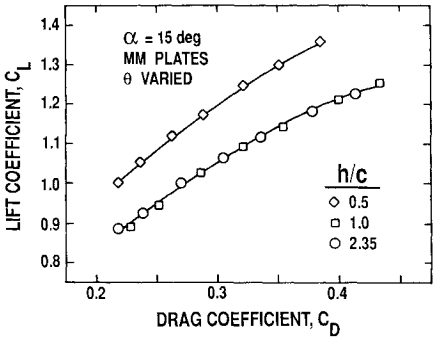

Fig. 7 Wing-in-ground effects on aerodynamic coefficients, α = 15 deg.

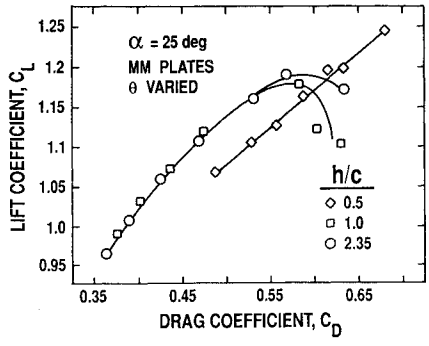

Fig. 8 Wing-in-ground effects on aerodynamic coefficients, $\alpha = 25$ deg.

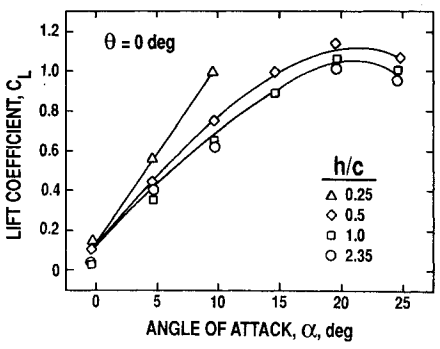

Fig. 11 Angle of attack and ground effects on lift coefficient.

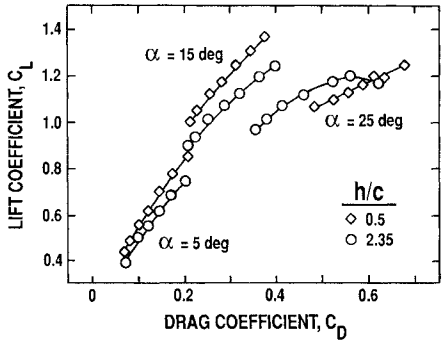

Fig. 9 Comparison of wing-in-ground effects on aerodynamic coefficients.

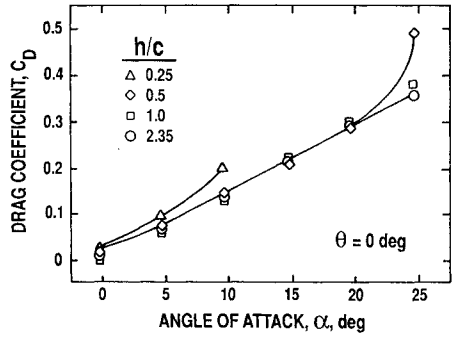

Fig. 12 Angle of attack and ground effects on drag coefficient.

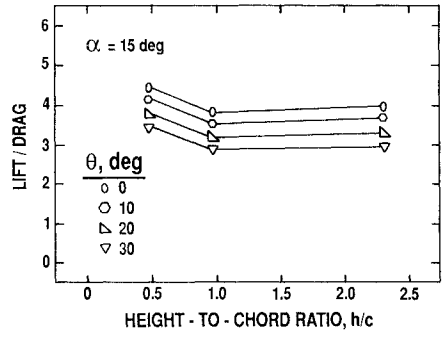

Fig. 10 Wing-in-ground effects on lift-to-drag ratio.

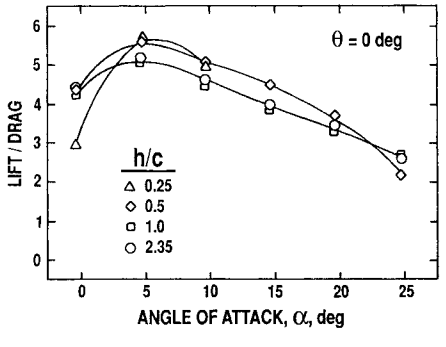

Fig. 13 Angle of attack and ground effects on lift-to-drag ratio.

sized plates are shown for three different values of α and several values of h/c in Figs. 6–8. The plots were generated by varying the flap angle θ from 0 to 30 deg. The polar curve for $h/c = 0.25$ in Fig. 6 is equivalent to the results with plates shown in Figs. 3 and 4. The lift and drag advantages due to WIG effects is apparent in Figs. 6 and 7 for $h/c < 1$. At $h/c = 1$ and 2.35, the polar curves were the same, which indicates WIG effects only for values of $h/c < 1$. Results at $\alpha = 25$ deg in Fig. 8 show that for any θ both C_L and C_D were higher at $h/c = 0.5$ compared with the coefficients at $h/c = 1$ and 2.35. The results at $h/c = 0.5$ and 2.35 in Figs. 6–8 are replotted in Fig. 9 to compare the WIG effects at different angles of attack.

The results in Fig. 7 are also replotted in Fig. 10 to show the lift/drag ratio as a function of h/c for four different values of flap angle θ. The increased lift/drag ratio for $h/c < 1$ is illustrated. These results, as well as those indicated previously, showed that it was advantageous to have end plates up to $h/c = 1.0$ but not necessarily at higher values of h/c. In actual practice, however, the end plates can be withdrawn like the landing gear when they become ineffective. As described by Chawla,[2] end plates act as containment walls for the air flow being forced under the wing by thrust vectoring and/or the forward speed of the vehicle. They also serve as a vehicle support system at rest, or at slow speeds, by developing an air cushion underneath the vehicle. The end plates could replace the landing gear but their use as a landing gear would probably entail the design of a special ground handling system to move the aircraft around.[2]

The lift coefficient and drag coefficient as a function of angle of attack α for $\theta = 0$ are shown in Figs. 11 and 12, respectively, for four values of h/c. Typical lift coefficient curves were obtained showing that separation occurred at the higher values of α. The results further illustrate that the lift

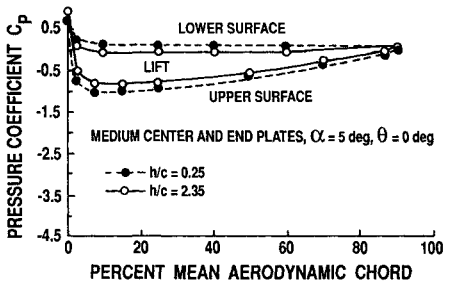

Fig. 14 Comparison of pressure profiles.

and drag coefficients were affected by WIG effects at $h/c = 0.25$ and 0.5. The corresponding lift-to-drag ratio curves are shown in Fig. 13. These results for zero flap angle showed the lift-to-drag ratio varied with α and that the higher values due to WIG effects were limited to an intermediate α range.

Wing pressure profiles on the upper and lower surfaces are shown in Fig. 14 for $h/c = 0.25$ and 2.35. The increased lift is apparent for $h/c = 0.25$ compared with that for $h/c = 2.35$. These results are typical of the pressure profiles obtained for other test conditions.

Conclusions

Wing-in-ground effects at values of $h/c < 1$ and at angles of attack below stall resulted in an increased lift coefficient for a given drag coefficient and an increased lift-to-drag ratio compared with freestream values. Freestream values were approached in the vicinity of $h/c = 1$ or heights above the ground of 1 c. The use of end plates resulted in an increased lift-to-drag ratio when the wing was within ground effects. At $h/c = 0.25$ the plates increased the lift coefficient by approximately 15%, whereas at $h/c = 0.5$ and $h/c = 1$, the plates only increased the lift coefficient by a maximum of 7 and 4%, respectively. End plate heights that differed by as much as 0.08 c did not change WIG effects significantly. The effect of the end plates was about the same with or without center plates. Pressure profiles on the upper and lower wing surfaces showed general agreement with the lift results obtained from the balance. The results should be useful to other WIG effect studies and particularly for further studies of the power-augmented ram, WIG effect launcher.

References

[1]Thomas, J. L., Paulson, J. W., Jr., and Margason, R. J., "Powered Low-Aspect-Ratio Wing In Ground Effect (WIG) Aerodynamic Characteristics," NASA TM-78793, July 1979.

[2]Chawla, M. D., "Horizontal Launch System for Transatmospheric Vehicles," 1987 International Air Cushion Technology Conference, Montreal, Quebec, Canada, Sept. 1987.

[3]Edwards, L. C., "Experimental Study of Wing-in-Ground Effects in the AFIT 5-foot Wind Tunnel," M.S. Thesis, School of Engineering, Air Force Institute of Technology, Wright-Patterson Air Force Base, OH, AFIT/GAE/AA/87M-1, March 1987.

[4]Gallington, R. W. and Miller, M. K., "The RAM-Wing: A Comparison of Simple One-Dimensional Theory with Wind Tunnel and Free Flight Results," AIAA Paper No. 70-971, August 1970.